2012

Fiber Type and Cross-Sectional Area Characteristics in Hindlimb Muscles of the Long-Lived Ames Dwarf Mouse

Kristine Dahlheimer
University of North Dakota

FIBER TYPE AND CROSS-SECTIONAL AREA CHARACTERISTICS IN HINDLIMB MUSCLES OF THE LONG-LIVED AMES DWARF MOUSE

by

Kristine Dahlheimer

A Scholarly Project Submitted to the Graduate Faculty of the

Department of Physical Therapy

School of Medicine

University of North Dakota

in partial fulfillment of the requirements for the degree of

Doctor of Physical Therapy

Grand Forks, North Dakota
May, 2012

This Scholarly Project, submitted by Kristine Dahlheimer in partial fulfillment of the requirements for the Degree of Doctor of Physical Therapy from the University of North Dakota, has been read by the Advisor and Chairperson of Physical Therapy under whom the work has been done and is hereby approved.

_____
(Graduate School Advisor)

_____
(Chairperson, Physical Therapy)

PERMISSION

Title Fiber Type and Cross-sectional Area Characteristics in Hindlimb Muscles of the Long-lived Ames Dwarf Mouse

Department Physical Therapy

Degree Doctor of Physical Therapy

In presenting this Scholarly Project in partial fulfillment of the requirements for a graduate degree from the University of North Dakota, I agree that the Department of Physical Therapy shall make it freely available for inspection. I further agree that permission for extensive copying for scholarly purposes may be granted by the professor who supervised my work or, in his absence, by the Chairperson of the department. It is understood that any copying or publication or other use of this Scholarly Project or part thereof for financial gain shall not be allowed without my written permission. It is also understood that due recognition shall be given to me and the University of North Dakota in any scholarly use which may be made of any material in this Scholarly Project.

Signature _____

Date _____

TABLE OF CONTENTS

LIST OF FIGURES

LIST OF TABLES

ACKNOWLEDGEMENTS

I would like to personally acknowledge and thank my research partner David Farder. This research project was a group effort during laboratory activities, analysis and paper writing. I appreciate the companionship and friendship that has grown due to this experience.

I would also like to express gratitude to Dr. Mark Romanick, my graduate advisor, for all of his help during laboratory procedures as well as input and critique during the development of this paper.

I want to thank Holly Brown-Borg for the utilization of her laboratory, laboratory supplies and colony of mice, throughout the entirety of the research. A special thanks to Sharlene Rakoczy for all of her patience and laboratory advice.

I am also grateful for my family, especially my parents, they have been extremely supportive and encouraging throughout my academic career.

ABSTRACT

Background: Ageing is associated with sarcopenia and a change of composition in muscle fibers. Ames dwarf mice have been found to have a decreased susceptibility to the deleterious effects of the ageing process, when compared to a normal mouse counterpart. This study looks at the muscle composition of the Ames dwarf mouse compared to the normal mouse by analyzing two muscles, ELD and Sol.

Methods: Researchers harvested hind limb muscles from Ames dwarf mice and normal mice. The fours muscles were EDL, Sol, Gastrocnemius/Plantaris, and TA. EDL and Sol were sliced and stained with fast and slow twitch and H&E stains. Muscle cell diameter and fast and slow twitch percentage were measured through images obtained.

Results: The following results were obtained using SPSS, version 18. For EDL, no significant difference was found between age of mice. A sig diff was found when comparing the total means of the type of mice. For Soleus, a significant interaction was found ($p<.001$) between mouse types and age. A significant difference in mouse types(dwarf and normal) was found at 3 months and also 12 months. A significant difference was found between normal mice at 3 and 12 months, while no significant difference was found between dwarf mice at 3 and

12 months. Percentages of fast and slow twitch muscle fibers were documented. No statistical analysis was used to determine significance.

Discussion: These results suggest that there are physiological differences between normal and Ames dwarf mice. Researchers expected to find a significant decrease is muscle cell diameter as the mouse aged; however, results showed that the muscle cell diameter actually increased with age. This may be due to the mouse not reaching full maturity during the age groups used in this study. The Further research is needed to substantiate the results of this study. Researchers suggest analyzing age groups of 24 months.

LITERATURE REVIEW

The course of aging results in numerous changes in the body, occurring throughout all systems. Around the age of 50, muscle mass decreases 1% to 2% annually, with a change in muscle strength of 1.5% between 50 and 60 years old and 3% annually after age 60.[1,2] Rosenberg[3,4] proposed the term for age-related decrease in muscular mass as "sarcopenia," from the Greek meaning "poverty of flesh." Since Rosenberg coined the term sarcopenia, there has been a change in the definition. The current working definition for sarcopenia is defined as: the loss of skeletal muscle mass and strength that occurs with advancing age.[5]

In order to obtain a clinical diagnosis of sarcopenia the European Working Group on Sarcopenia in Older People (EWGSOP) recommends the following conditions for a diagnosis: three criteria, of which two are needed for a diagnosis, criterion one (low muscle mass) and either criterion two (low muscle strength) or three (low physical performance).[3,4,5,6] EWGSOP also categorizes sarcopenia in stages noted in Table 1. The criteria can be assessed using numerous techniques based upon the availability and suitability of the research and clinical setting. Muscle mass analysis may consist of bioimpedance analysis (BIA), total or partial body potassium per fat-free soft tissue, anthropometric measures, and body imaging techniques, such as computed tomography (CT scan), magnetic resonance imaging (MRI), and dual energy X-ray absorptiometry (DXA). Muscle

strength can be determined by handgrip, knee flexion/extension or peak expiratory flow. Physical performance can be assessed with Short Physical Performance Battery (SPPB), gait speed, timed get-up-and-go test (TGUG), or a stair climb power test.[6]

Table 1. EEGSOP Conceptual Stages of Sarcopenia[6]

Stage	Muscle mass	Muscle strength	Performance
Presarcopenia	↓		
Sarcopenia	↓	↓ **Or**	↓
Severe Sarcopenia	↓	↓	↓

Muscle tissue can be categorized into three types (skeletal, cardiac, and smooth) based on various characteristics specific to each type; however, the general cellular structure is similar in all muscle. Numerous structures are involved in the formation of muscles. The following is a brief description of a macroscopic to microscopic description of skeletal muscle structures.

Skeletal muscle bellies can be divided into numerous layers which are encased by fibrous connective tissue or fascia (epimysium, perimysium, and endomysium). The muscle belly is surrounded by epimysium. The muscle belly is further divided into fascicles, bundles of muscle fibers (cells), and surrounded by perimysium. Blood vessels and nerves are also encased within the perimysium sheath. Each individual muscle fiber is surrounded by endomysium which allows for the individual movement of the muscle cells; this is also the location for metabolic exchanges between muscle fibers and capillaries. A muscle fiber

consists of multiple nuclei, mitochondria, and myofibrils. Myofibrils consist of myofilaments (actin, and myosin) which are contractile proteins of the muscle cell. These myofilaments form a structure called a sarcomere. Sarcomeres are the contractile unit of muscle fibers, which are present continuously through the length of the muscle fiber. The boundaries of sarcomeres are described by the location between the z-lines/z-disks. Noncontractile proteins comprise a majority of the cytoskeleton within and between muscle fibers, giving support throughout the muscle.[7] Figure 1 is a pictorial depiction of the macroscopic and microscopic units of skeletal muscle.

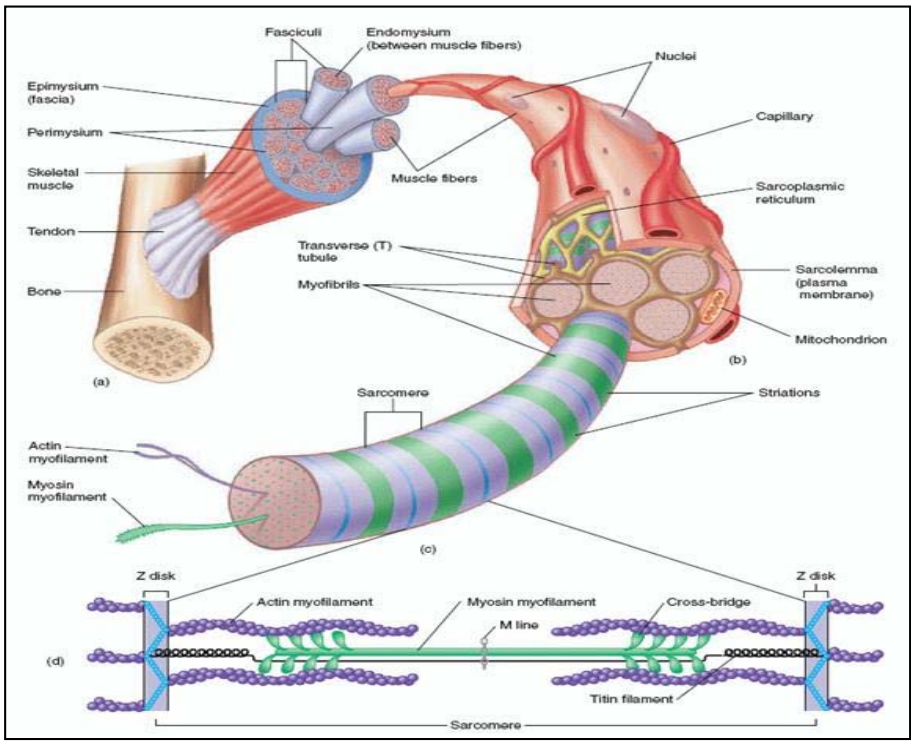

Figure 1. Components of Skeletal Muscles[8]

Muscle cells are innervated by alpha motor neurons. A single alpha motor neuron and the multiple fibers it innervates is called a motor unit. Motor units can be broken down into three types: slow, fast fatigue-resistant, and fast fatigable. The types of muscle fibers vary in the speed of contraction as well as resistance to fatigue. These differences are due to the histochemical profile of each fiber. There are two types of systems which comprise the histochemical profile, glycolytic and oxidative. Oxidative fibers have a smaller cellular diameter, higher percentage of mitchondria, and require oxygen for functioning; therefore these fibers are slow contracting but fatigue resistant. Glycolytic fibers have a large cellular diameter, lower percentage of mitochondria and require minimal oxygenation for functioning; therefore, these fibers are fast contracting and quickly fatigue.[9] One muscle type is a combination of the two histochemical profiles, fast oxidative glycolytic; therefore the functional capacity of this fiber is in between the two other types. Muscle fibers involving slow motor units are generally fatigue resistant, often known as slow twitch fibers, which utilize a slow oxidative histochemical profile. Motor units that are fast and brief consist of fast fatigable fibers, which have a high amplitude contraction but rapidly fatigue. The histochemical profile of these fibers is fast glycolytic. Fast fatigue-resistant fibers are an intermediate motor unit that utilizes a fast oxidative glycolytic system. These fibers have a longer contractility component compared to the fast fatigable fibers but are unable to maintain the endurance of the slow motor units. Table 2 compares the classification of the three motor unit and fiber types.

Table 2. A Comparison of Three Methods of Fiber Typing Skeletal Muscle[7]		
Motor Unit Types	**Histochemical Profile of fibers based on relative oxidative or glycolytic metabolism**	**Histochemical profile of fibers based on relative activity of myosin ATPase**
Slow	Slow oxidative	Type I (low activity)
Fast fatigue-resistant	Fast oxidative glycolytic	Type IIA (high activity)
Fast fatigable	Fast glycolytic	Type IIX (high activity)

Throughout one's lifetime muscles experience structural changes; these changes consist of decreased quality of slow and fast motor units with an accelerated loss of fast motor units, fiber atrophy, and decreased cross-sectional area. Muscle denervation causes a loss of functional motor units, increasing the work of the current innervated motor units. The surviving motor units, typically Type I fibers, are able to recruit denervated fibers, resulting in a physiological change of the reinnervated muscle fibers to that of the current innervating motor unit, increasing the percentage of type I fibers in the cross sectional area.[10] The resultant loss of type II fibers is attributed to the decrease in muscle power associated with aging. Another aging process affecting muscles is the increased deposition of adipocytes within the muscle tissue.[10] These are a few of the numerous changes muscles undergo during the aging process.

Sarcopenia is experienced by males and females and is clinically associated with decreased health outcomes and increased disability.[11] According to the Baumgartner et al[12] study performed on 883 elderly Hispanic and non-Hispanic males and females in New Mexico, women with sarcopenia had a 3.6

times higher rate of disability compared to individuals without sarcopenia. Males were found to have a 4.1 times higher disability rate compared to males with normal muscle mass.

There are multiple mechanisms attributed to sarcopenia, which affect the onset and progression of the diagnosis. An improved understanding and intervention of these associated factors will direct research to determine appropriate preventative strategies for sarcopenia. Figure 2 is a flow chart describing conditions which have an effect on the process of sarcopenia.[6]

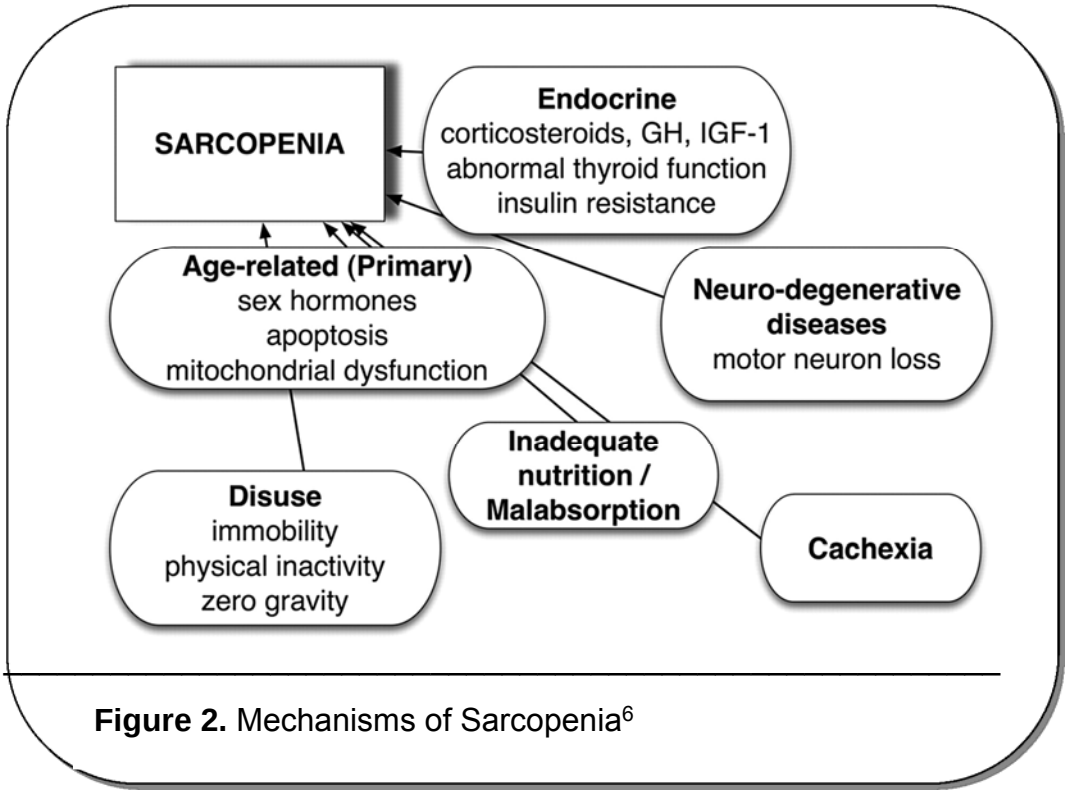

Figure 2. Mechanisms of Sarcopenia[6]

Another factor in aging has been associated with free radicals. According to Taber's Cyclopedic Medical Dictionary a free radical is "a molecule containing an odd number of electrons. These molecules contain an open bond or a half bond and are highly reactive…the body has developed methods of defending against the harmful effects of free radicals. Superoxide dismutases, enzymes within the mitochondria and antioxidants are effective in counteracting the harmful effects of free radicals."[13] Denham Harman[14] is acknowledged as the first individual to attribute free radicals to the degradation of cells. Free radicals are formed when OH and HO_2 are dissociated from molecules. Harman noted that a likely source of OH and HO_2 radicals is involved in the interaction of respiratory enzymes and molecular oxygen. The conversion of hydrogen peroxide (H_2O_2) can form two distinctively different compounds: water (H_20) or hydroxyl radical (OH-). The free radical OH- has been attributed to the breakdown of hemoglobin and myoglobin.[14] Free radicals are associated with decreased cellular signaling which has a negative effect on all of the body's systems. Free radicals are associated with disease processes, but further research is required to determine if the redox signaling is a cause or an association with certain diseases. [15]

The free radical theory has evolved since 1956, also evolving the name of the theory to oxidative stress theory. The current theory notes oxidative stress exists in all basal conditions of aerobic organisms due to an imbalance of proxidants and antioxidants, resulting in a gradual accumulation of oxidative damage in various macromolecules throughout the system. Damage caused by oxidation increases with age, resulting in altered cellular processes.[16,17] An

overall increase in age is associated with a muscle-specific increased oxidative environment, decreasing the body's ability to compensate with antioxidants, resulting in increased oxidative damage. Skeletal muscles contain high concentrations of myoglobin, a macromolecule which readily converts hydrogen peroxide to other highly reactive oxygen species (ROS) increasing the exposure of free radicals to the surrounding molecules in skeletal muscle.[16]

The susceptibility to oxidative stress can be further described in skeletal muscles by the histochemical profile of the various fiber types. Type I fibers utilize an oxidative metabolism which produces a greater number of ROS via mitochondrial oxidative phosphorylation compared with type II fibers. Due to the increased basal production of ROS type I fibers have an increased basal antioxidant defense compared with type II, allowing type I to have a higher antioxidant capacity, which decreases the muscle tissue's susceptibility to oxidative stress.[16] Reactive protein carbonylation can be used as a prominent marker for oxidative stress in skeletal muscles. Protein carbyonylation occurs mainly through two mechanisms, metal-catalyzed oxidation and reactions between nucleophilic amino acid side chains and lipid oxidation products. Thompson[16] researched the differences in type I and type II fibers in relation to the mitochondrial protein carbonylation. Type II muscles experienced about two times greater protein carbonylation susceptibility, with a significant increase with aging when compared to type I.[16] This large increase in oxidative stress in type II fibers may contribute to the impaired cellular function in aged type II muscle fibers.

It is important to note that an excessive amount of free radicals can lead to oxidative stress and cellular damage; there are also a few advantageous effects of free radicals. Reports have been given describing the association of free radicals and enhanced signal transduction, sensing of oxygen tension, and reduction of vascular tone.[18] Oxidative damage can be decreased/countered due to endogenous enzymatic and nonenzymatic defense mechanisms consisting of but not limited to catalase, glutathione peroxidase (GPX), superoxide dismutase, glutathione, ascorbic acid, and metallothionein.[18] This evidence supports the maintenance of cellular muscular homeostasis even in the presence of ROS.

Ames dwarf mice have (*df/df)* have demonstrated an increased antioxidant defense, which has been displayed across numerous tissues.[18, 19, 20] Ames dwarf mice have a proline point mutation in the α 1 helix of the transcription factor on chromosome 11 with a resulting extreme decrease or absence in anterior pituitary cells which normally produce and secrete growth hormone (GH), prolactin, and thyroid stimulating hormone (TSH),[18, 21] resulting in a deficiency in GH, prolactin, and TSH. Comparing Ames dwarf mice to their normal wild type siblings, male and female dwarf mice live significantly longer ($p<.0001$) than the wild type. On average a difference of 350 days between the males and 470 days between the females appears when comparing the two mouse types resulting in an improved lifespan of 50% to 70%.[20, 21]

CHAPTER II

METHODS

Subjects

Over the course of four dates of dissection, we used a total of 7 mice; 4 were genotypically normal(wild type,N) and 3 were Ames Dwarf Mice(df). The animals were taken from a colony bred at the University of North Dakota. Age ranged from 3 months old to 12 months old. See Tables 1 and 2 for mouse specific age, weight, and genotype. To safely handle the subjects, each researcher completed a course in Animal Care and Use from the AALAS Learning Library.

Skeletal Muscle Tissue Acquisition

Prior to tissue extraction, setting up the lab was as follows. We pre-labeled eight small test tubes for each mouse, one for each muscle. Abbreviations for muscles are as follows; Sol = Soleus, GP = Gastrocnemius and Plantaris, TA = Tibialis Anterior, EDL = Extensor Digitorum Longus. A genotypically normal mouse was labeled N1, N2, etc. The Ames Dwarf was labeled df3, df4, etc due to previous labeling in a parallel study.

Each mouse was weighed using a standard laboratory scale. See Table 1 for individual weights. Dissection began with using 300 or 400 µl of tribromoethanol

(2.5% in 0.9% saline) for N, and 100 µl for df injected in the peritoneal cavity. Pain reflexes were checked by squeezing feet and checking corneal reflexes . These reflexes were checked periodically to ensure the mouse was properly sedated. Additional increments of 100 µl were injected throughout the procedure as needed based on subject response to these reflexes. See Table 1 for the amount of tribromoethanol used for each mouse. Circumferential incisions were made around the ankle to free hindlimb skin. Scissors or forceps were used to separate the skin from underlying structures. An incision was made from the ankle running cranial to the hip joint, peeling the skin from the tissues beneath. The following muscles were identified based on their anatomical position and physiological action: soleus (Sol), gastrocnemius and plantaris (GP), tibialis anterior (TA), extensor digitorum longus, (EDL). The distal attachment of GP/Sol was cut at the heel, as close to the bone as possible. It was retracted proximally and Sol was separated from the GP complex using forceps. Sol proximal attachment was then severed, and Sol was weighed. These findings are documented in Table 2. Sol was then covered in Optimal Cutting Temperature compound (OCT) and placed flat and straight on a section of the previously acquired liver to maintain physiological fiber orientation. OCT was used again to cover both the liver and Sol. This was then placed on a creased weight boat fragment to later locate muscle orientation and submerged for five seconds in isopentane that was cooled in liquid nitrogen. Then it was placed in an appropriately labeled test tube and kept cold in liquid nitrogen. GP was cut and the proximal attachment at the knee and weighed. It was then dipped in

isopentane for five seconds and placed in a test tube and then in liquid nitrogen. The TA was separated from the underlying fascia and bone, sliding along the tibia. The distal attachment was cut and then retracted and cut again at the proximal attachment. TA was processed similar to GP. EDL was separated from surrounding tissues, and cut at the distal and then proximal attachments. EDL was treated similarly to Sol with liver, OCT, weight boat fragment, and freezing. Length was taken for N4 and df5 muscles using a standard 12 inch ruler, with metric markings. These findings are documented in Table 2. This entire procedure was performed on the contralateral lower limb. After completion, all tissues were stored in a -80˚C freezer.

Tissue Slicing

A Micron HM 550 Cryostat machine (ThermoFischer Scientific, Walldorf, Germany) was used to perform tissue slicing. It was set at a temperature of -25˚C, and the cutting blade was cleaned with alcohol and set in the Cryostat 30 minutes prior to tissue slicing to allow appropriate time for the blade to cool. The tissue was placed in the Cryostat to reach the temperature of -25˚C. One muscle was sliced at a time. The muscle fibers were attached to the chuck with OCT, perpendicular to the cutting blade. Slices that were 50-µm thick were cut until muscle tissue was observed. Then 10-µm thick slices were used for the remainder in the procedure. Ten slides were made, each slide containing three tissue slices. Then 500 µm were sliced and discarded. Another ten slides were made. This process was repeated until all muscle tissue had been sliced. A fine-tipped paint brush was used to flatten curled tissue slices on the slicing platform

for smooth transfer to the slides. Appropriate protocol was used from Cryostat maintenance following completion. The obtained slides were stored in -4˚C refrigerator.

Hematoxylin and Eosin Stain

The hematoxylin and eosin stains identify the number and position of the nuclei found in the muscle cross sectional area which demonstrates the location of cytolitic vs nuclear material.

The slides were removed from the refrigerator, and allowed to warm to room temperature. The slides were dipped in Harris hematoxylin for 2 minutes, then rinsed in distilled water twice. The slides were dipped three times in acid alcohol, which consists of 11 ml of glacial acetic acid, 95 ml ethanol, and 5 ml distilled water. The slides were rinsed in distilled water. Slides were dipped six times in ammonium water, which consists of 0.625 ml of 25% ammonium hydroxide in 250 ml distilled water. The slides were again rinsed in distilled water, then dipped for 30 seconds in working eosin solution. The working eosin solution consisted of the following:

Working Eosin		
Stock Eosin	200ml	62.5 ml
80% ethanol	600 ml	187.5 ml
Glacial Acetic Acid	5ml	1.56 ml

Eosin Stock	
Eosin Y	10 g
95% Ethanol	800ml
Distilled Water	200 ml

Slides were rinsed in distilled water twice, and dehydrated in ethanol for 15 seconds, once each in the following concentrations: 70%, 95%, 100%. After

clearing the slides in xylene, the slides were covered with Permount and a cover slide. The slides were stored at room temperature.

Stain – Fast and Slow twitch Fibers

The slides were stained with the following chemical kits to determine the location and number of fast and slow twitch muscle fibers. The following kits were used in this procedure; Vector Laboratories VECTOR® M.O.M.™ Immunodetection Kit, Vector® Laboratories Antibody to Myosin Heavy Chain (slow) and Vector® Laboratories Antibody to Myosin Heavy Chain (fast), Vector® Avidin/Biotin Blocking Kit, Vector ® DAB Substrate Kit(Vector Laboratories, Inc. US Headquarters, 30 Ingold Road. Burlingame, CA, 94010). The slides were removed from the -4˚C refrigerator and allowed to warm to room temperature.

10X Phosphate Buffered Saline (PBS)	
Distilled Water	900 ml
Sodium Phosphate Dibasic(Na_2HPO_4)	11.4 g
Sodium Chloride (NaCl)	90.0 g
Potassium Phosphate Monobasic (KH_2PO_4)	2.65 g
Potassium Chloride (KCl)	2.0 g

Once the salts were dissolved, the solution was brought to a final volume of 1000 ml with distilled water. The pH was maintained between 6.7 and 6.8. The working PBS solution (1X PBS) was created by mixing 100 ml 10X PBS with 900 ml distilled water, creating a pH of 7.4.

On the room-temperature slides, the tissue sections were encircled by using a PAP pen. Slides were rinsed by dipping in 1X PBS solution for two minutes. Excess PBS was removed by lightly shaking the slides and placed in a pan.

The H_2O_2/horse serum (30µl H_2O_2 + 9µl horse serum in 3 ml PBS) was mixed. Each tissue section was covered with this solution. A small pipette tip was used to completely cover the tissues with this serum and incubated for five minutes. Excess serum was shaken off and the slides were rinsed in 1X PBS twice, for two minutes each time. The excess PBS was shaken off and the slides were positioned in a pan.

The tissue sections were completely covered with Avidin blocking solution for 15 minutes. The excess was shaken off and then rinsed in 1X PBS for two minutes. The excess PBS was shaken off. A solution containing 36 µl mouse IgG blocking reagent + 1 ml 1X PBS was mixed and then applied to the tissue sections. The slides were set in a small pan, and placed in a larger pan with a layer of water in the larger pan. This allowed for proper humidity during incubation. The slides were incubated for one hour.

The slides were rinsed in 1X PBS twice for two minutes each time and the excess was shaken off. The M.O.M. diluent was created by mixing 80 µl of protein concentrate + 1 ml 1X PBS and set aside for 5 minutes, and the excess was shaken off. Do not rinse.

One slide that will act as a control slide was removed. The remaining slides were divided into two groups, fast twitch and slow twitch.

Antibody solutions for each fiber type;
24 µl slow antibody + 456 µl of MOM diluent
47 µl fast antibody + 425 µl of MOM diluent

Using 100 µl of the above solutions, the slides were covered with their associated antibody; the slow twitch antibody was placed on the slides in the slow twitch muscle group. Slides were set in a pan, covered, and set aside for 30 minutes at room temperature. This step was not performed with the control slide.

All the slides, including the control, were then rinsed in 1X PBS twice for two minutes. The slides were then incubated in 4 µl of MOM Biotinylated Anti-Mouse IgG Reagent + 1 ml of MOM working diluent for ten minutes, and then rinsed in 1X PBS twice, for two minutes.

A solution of one drop of Reagent A and 1.25 ml 1X PBS was mixed using the vortex, and one drop of Reagent B was added and mixed using the vortex. This solution stood for 30 minutes at room temperature. (This can be prepared ahead of time.)

The slides were covered with Reagent A + B solution for 5 minutes, and rinsed in 1X PBS twice, for two minutes.

DAB solution;	
Distilled Water	2.5 ml
Buffer pH 7.5	one drop
DAB substrate reagent	two drops
H_2O_2 solution	one drop
Nickel solution	one drop

The slides were covered with DAB solution, and sat for ten minutes. Then they were rinsed for one minute in distilled water.

The remaining steps were completed under the laboratory hood. The slides were dehydrated by dipping them in 70% ethanol twice for 15 seconds. This step was repeated with 95% and 100% ethanol. Once more, the slides were dehydrated in xylene and covered with Permount solution and coverslips. The slides were placed flat and allowed to dry overnight.

Slide Imaging

An electronic camera and standard laboratory microscope were used along with imaging software. The 4X setting on the microscope was used when placing and removing slides from the platform. A slide was chosen and placed on the platform of the microscope. The image of the slide was focused using the 4X lens. The microscope was moved to the 10X lens and then the slide was properly positioned for the most optimal cross-sectional picture. Using the computer software, a picture was taken using color parameters that provided the clearest photograph. The color scheme utilized in this study was Red = 1.569, Green = 1.000, Blue = 2.276. One picture from each slide was captured.

Cross-sectional Area

Scion software (http://www.scioncorp.com/) was used in this study, and the calibration performed here was done with a 1000 μm ruler. Using the printed image of the tissue section, a cross sectional area of the muscle was determined to be measured. The associated cells were individually measured utilizing a freehand tool on the computer and marked accordingly on the printed image to prevent error in cell circling. The data gathered from each individual muscle cell was saved in a corresponding table, and the average individual cross-sectional

area was determined. The sum of each individual cross-sectional area was compared to entire diameter of all the cells, to determine accuracy of individual cell circling.

CHAPTER III

RESULTS

The following Table 1 values were gathered from the respective animals during surgery. See Table 2 for information gathered during the procedure as mentioned in Methods. Muscle weight and length were obtained for each mouse used in the study. Due to protocol alterations, muscle weight and length for certain animals was not documented. Also note df3 GP was not weighed due to anatomical anomaly, and researchers were not able to identify this muscle during surgery.

Table 3. Animal Identification

Subject	Age	Animal Weight	Tribromethenol
N1	3 months	30.0 g	1000 ml
N2	3 months	30.9 g	900 ml
N3	3 months	29.01 g	700 ml
N4	12 months	37.7 g	800 ml
Df3	3 months	9.71 g	200 ml
Df4	3 months	9.382 g	200 ml
Df5	12 months	11.245 g	150 ml

Table 4. Muscle Data						
Subject	Right Muscle	Muscle weight (g)	Muscle Length (mm)	Left Muscle	Muscle Weight (g)	Muscle Length (mm)
N1	Sol			Sol		
	GP			GP		
	TA			TA		
	EDL			EDL		
N2	Sol	.010		Sol	.011	
	GP	.145		GP	.127	
	TA	.032		TA	.041	
	EDL	.007		EDL	.014	
N3	Sol	.014		Sol	.013	
	GP	.142		GP	.133	
	TA	.044		TA	.031	
	EDL	.012		EDL	.009	
N4	Sol	.021	11.5	Sol	.011	13.0
	GP	.128	16.0	GP	.133	14.0
	TA	.049	10.0	TA	.020	11.0
	EDL	.014	11.5	EDL	.012	12.0
Df3	Sol	.002		Sol	.003	
	GP	--		GP	.038	
	TA	.011		TA	.019	
	EDL	.001		EDL	.008	
Df4	Sol	.002		Sol	.003	
	GP	.045		GP	.038	
	TA	.020		TA	.028	
	EDL	.013		EDL	.003	
Df5	Sol	.018	3.5	Sol	.014	10.0
	GP	.055	7.0	GP	.042	9.0
	TA	.016	7.0	TA	.024	7.0
	EDL	.014	6.0	EDL	.013	9.0

Statistical analysis was performed with SPSS version 18.0, Chicago, IL. A Two-Way ANOVA test was utilized for all parametric analyses involving muscle cell diameter. Researchers found skewness was greater than the absolute value of 1.96, indicating the data was not evenly distributed. Due to this, a nonparametric test (Kruskal-Wallis Test) was performed to ensure that the null hypothesis could be rejected, and therefore a parametric could be used to analyze the data. A p-value of <.001 was found during the Kruskal-Wallis test, Table 5. The data in Table 6 was gathered by Scion Cell Circling software. Figure 3- 6 are examples of the H&E stain images that were utilized during cell circling.

Table 5. Statistical Hypothesis

Null Hypothesis	Test	Sig.	Decision
The distribution of area is the same across categories of all groups	Independent samples Kruskal-Wallis Test	.000	Reject the null hypothesis

Table 6. Mean and Standard Deviations				
Names	Age (months)	Muscle	Mean	Standard deviation
N5	>12	EDL	2286.022	1235.120
df5	>12	EDL	1342.716	569.071
N3	3	EDL	2576.556	1157.449
df4	3	EDL	1472.305	655.255
N4	>12	Sol	3258.491	913.769
df5	>12	Sol	1315.861	500.895
N2	3	Sol	2117.154	755.086
df4	3	Sol	1476.854	367.299

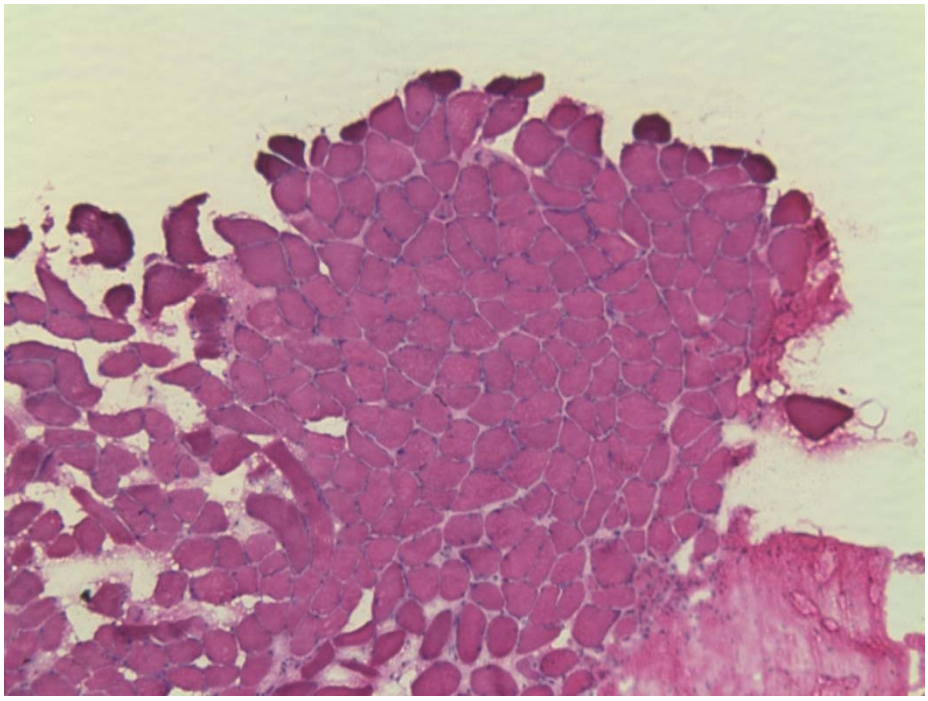

Figure 3. H&E Stain (N4 R Sol, 10x)

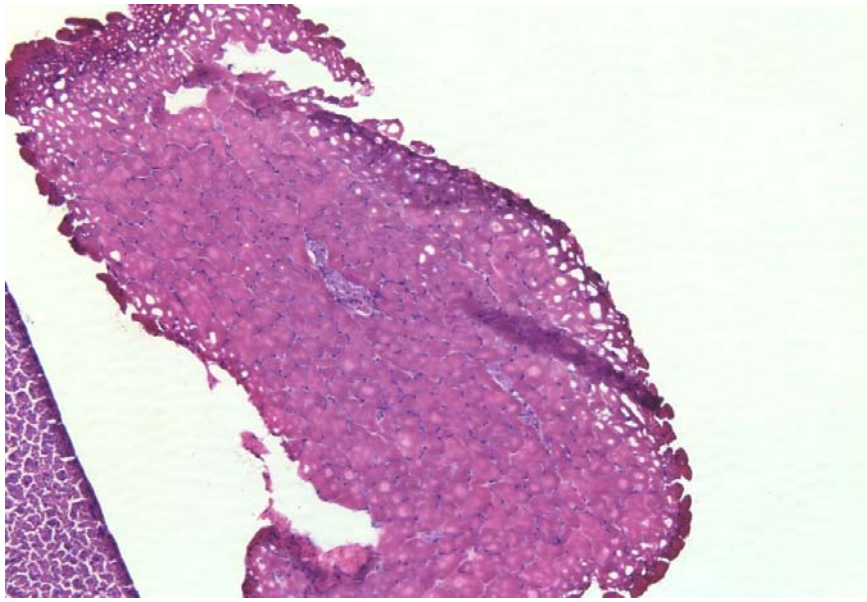

Figure 4. H&E Stain (df5 L Sol, 10x)

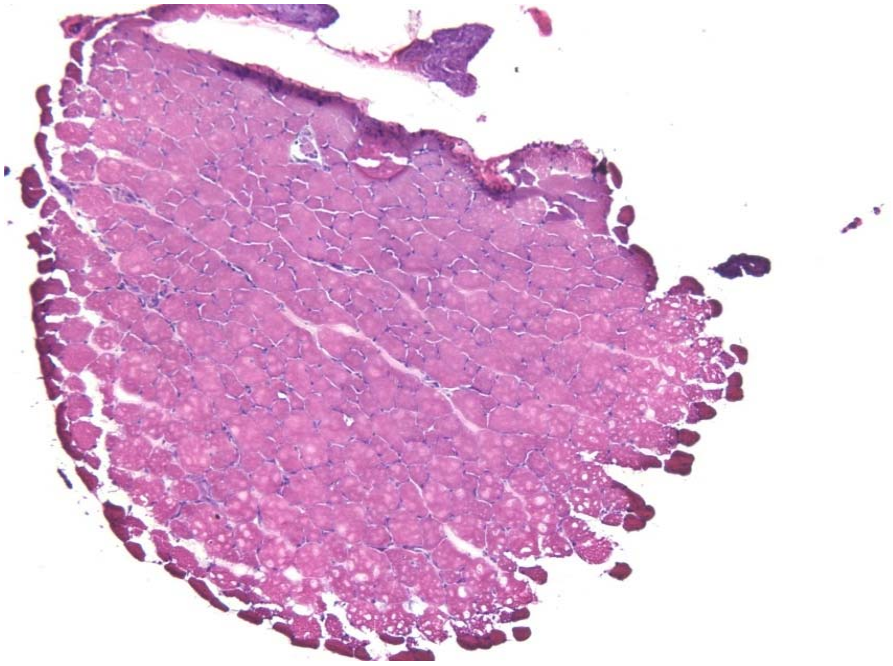

Figure 5. H&E Stain (df4 L EDL, 10x)

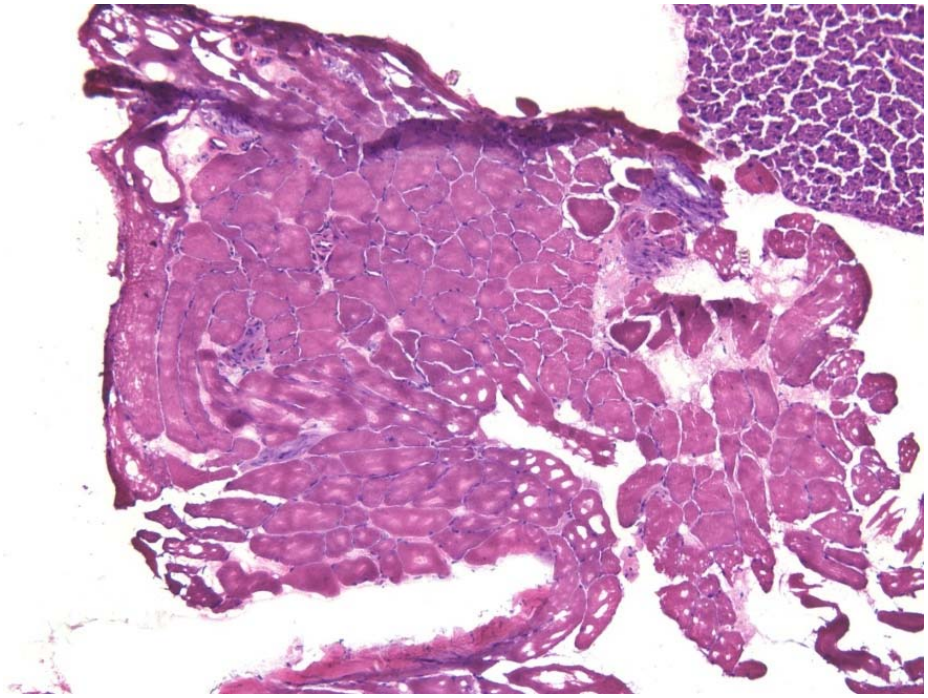

Figure 6. H&E Stain (N5 L EDL, 10x)

Analyzing EDL

Researchers found that there was no significant difference or interaction regarding cell diameter between age of the mice and the type, and no significant difference between the ages. There is a significant difference between the two types of mice, when comparing the total means. Total mean for the normal mouse was 2431.2890 μm and the dwarf mouse was 1407.5109 μm with a p-value < .001. See Table 7 for data and Figure 7 for pictorial analysis of significant differences

Table 7. EDL SPSS Data

Source	Type III Sum of Squares	df	Mean Square	F	Sig.	Partial Eta Squared	Observed Power[b]
mouse_#redo	4.717E7	1	4.717E7	52.139	.000	.229	1.000
age_redo	1985661.7	1	1985661.7	2.195	.140	.012	.314
mouse_#redo * age_redo	291412.44	1	291412.44	.322	.571	.002	.087
Error	1.592E8	176	904603.42				

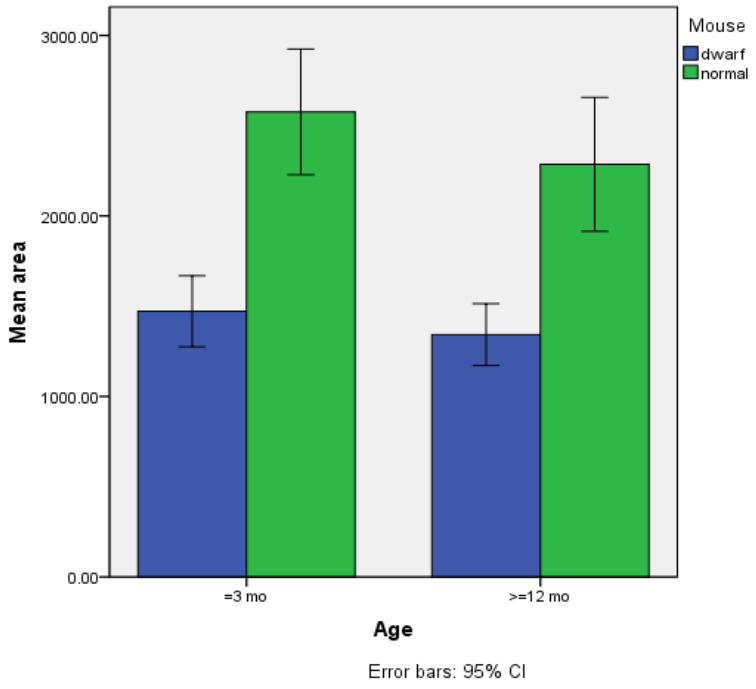

Figure 7. EDL Total Means

Analyzing Soleus

Researchers found a significant interaction between the mouse type and age, $p < .001$. See Table 8 for data obtained and Figure 8 for pictorial analysis of significant differences. Because there was a significant interaction, simple main effects were analyzed. Significant difference in mouse types was found at 3 months and also 12 months. Significant difference was found between normal mice at 3 and 12 months. No significant difference was found between dwarf mice at 3 and 12 months. See Figure 9 and 10.

Table 8. Sol SPSS Data

Source	Type III Sum of Squares	df	Mean Square	F	Sig.	Partial Eta Squared	Observed Power[b]
mouse_#redo	7.505E7	1	7.505E7	167.633	.000	.488	1.000
age_redo	1.081E7	1	1.081E7	24.148	.000	.121	.998
mouse_#redo * age_redo	1.908E7	1	1.908E7	42.616	.000	.195	1.000
Error	7.880E7	176	447733.281				

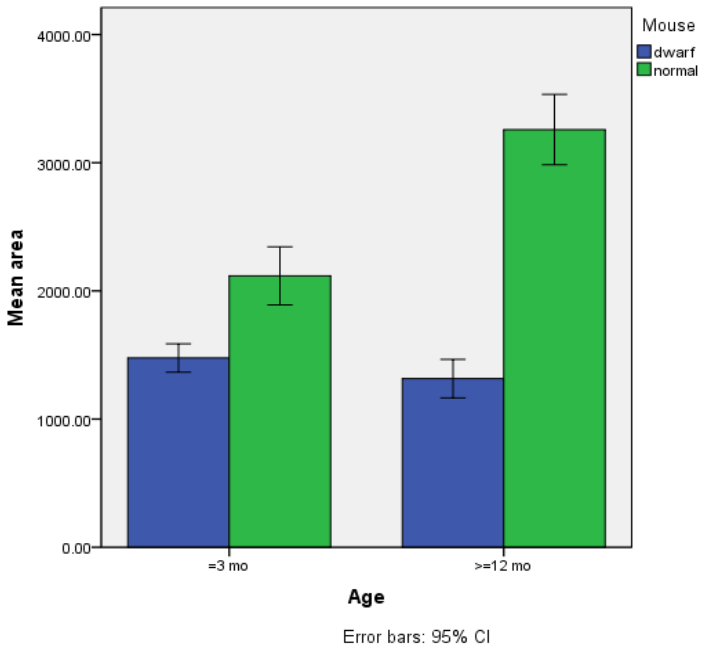

Figure 8. Sol Total Means

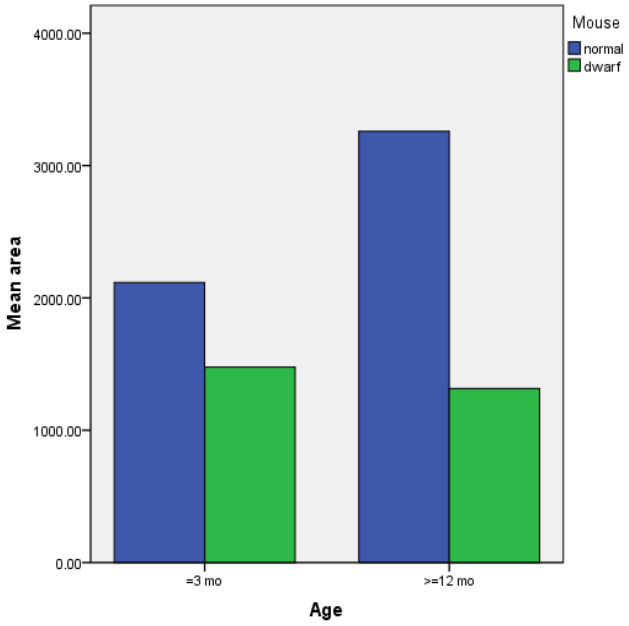

Figure 9. Simple Main Effects Between Mouse Type and Individual Age Groups

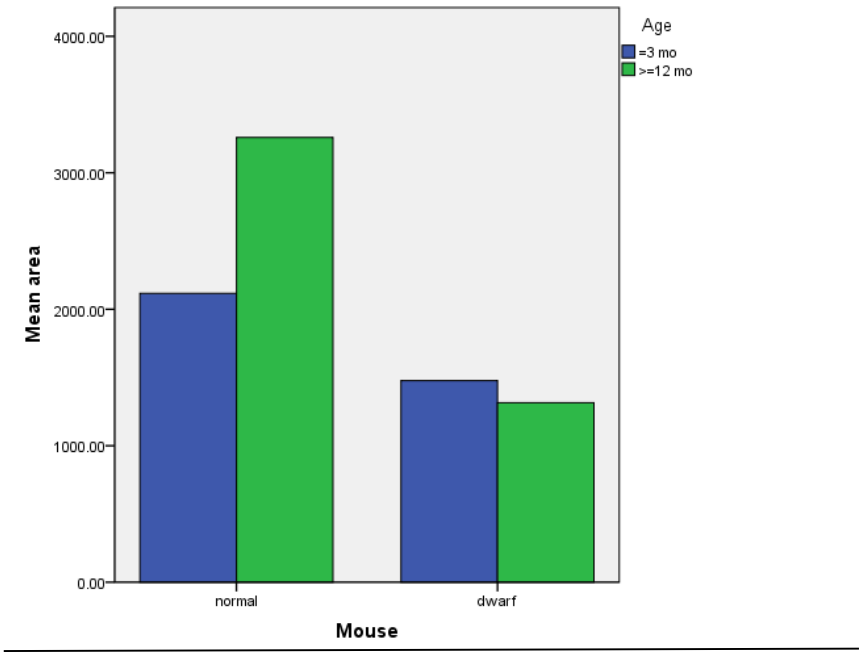

Figure 10. Simple Main Effects Between Mouse Type and Both Age Groups

Analysis of Muscle Fiber Types

The data in Table 9 was obtained by the pictures taken of the fast and slow twitch stained muscle slices. Data for df4_3 month_EDL and df5_>12 month_Sol was not obtained due to poor picture clarity. Figure 11- 18 are examples of the fast and slow twitch stain images.

Table 9. Fast and Slow Twitch Fiber Composition						
Age	**Muscle**	**Name**	**Fast**	**Percentage fast (%)**	**Slow**	**Percentage slow (%)**
3 month	SOL	df4	94/524	17.939	163/221	73.756
	SOL	N2	211/419	50.358	169/351	48.148
	EDL	df4			90/429	20.979
	EDL	N3	239/254	94.095	14/357	3.922
>12 month	SOL	df5			189/511	36.986
	SOL	N4	158/259	61.004	164/326	50.307
	EDL	df5	61/119	51.261	95/469	20.256
	EDL	N5	169/201	97.512	31/234	13.248

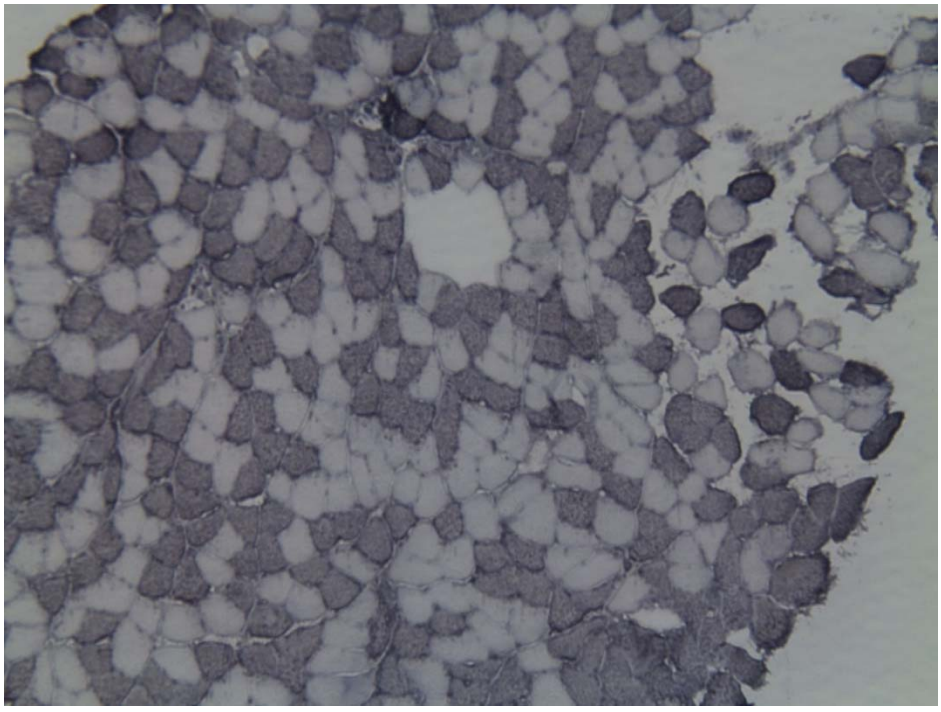

Figure 11. Fast twitch (N2 L Sol, 10x)

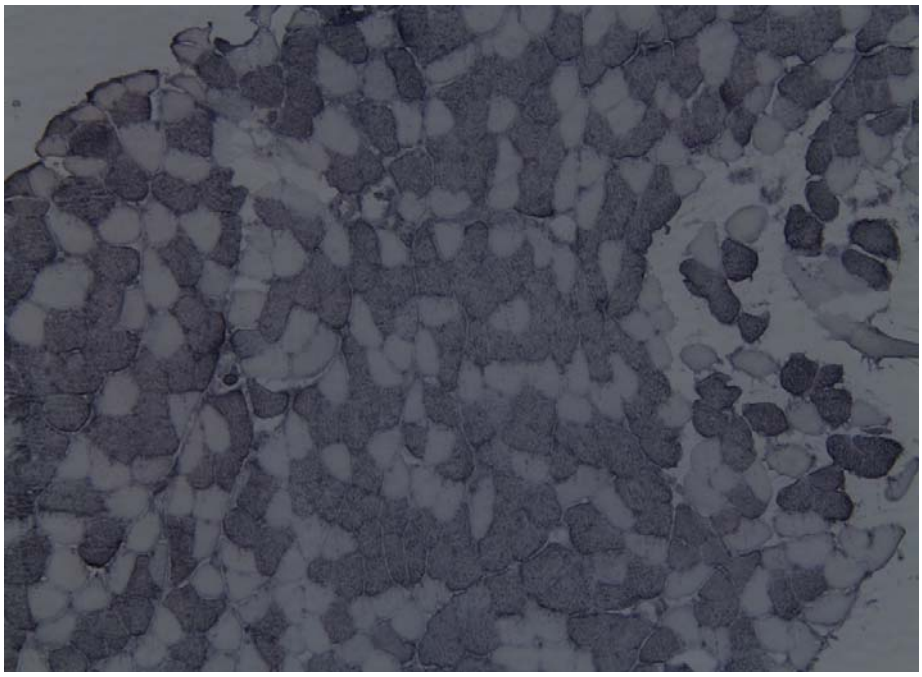

Figure 12. Slow twitch (N2 L Sol, 10x)

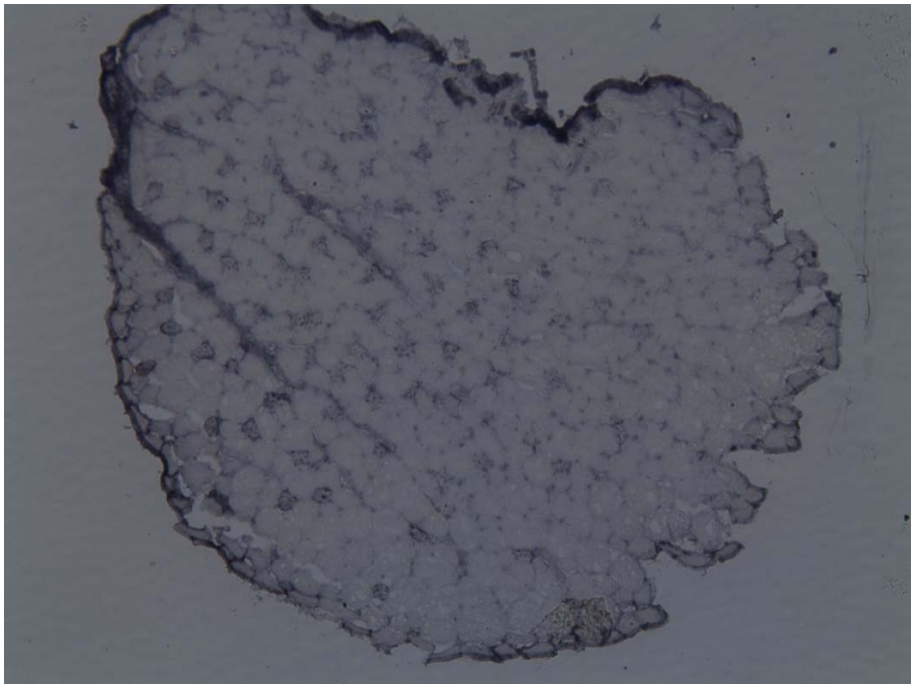

Figure 13. Slow Twitch (df4 L EDL, 10x)

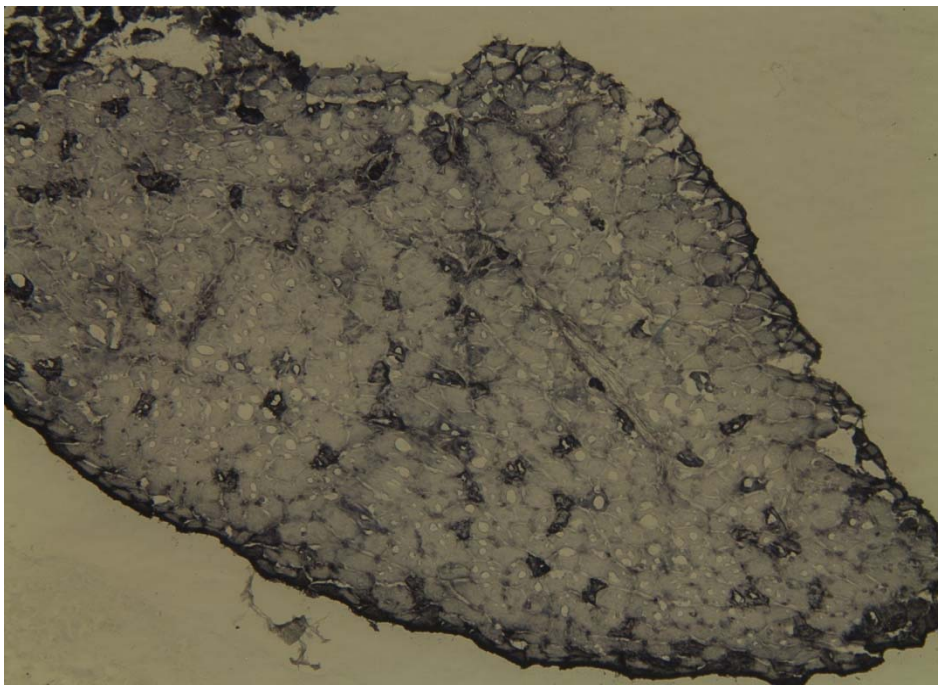

Figure 14. Fast Twich (df4 R Sol, 10x)

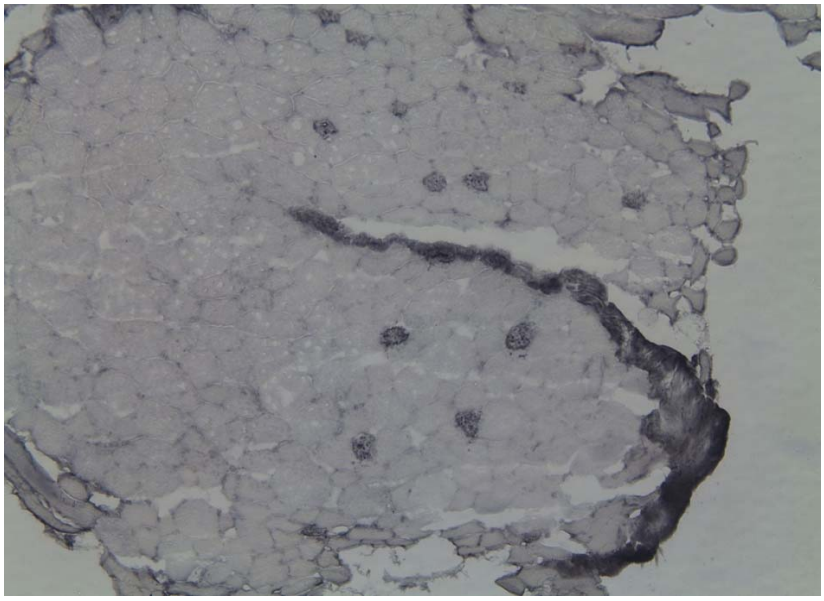

Figure 15. Slow Twitch (N3 R EDL, 10x)

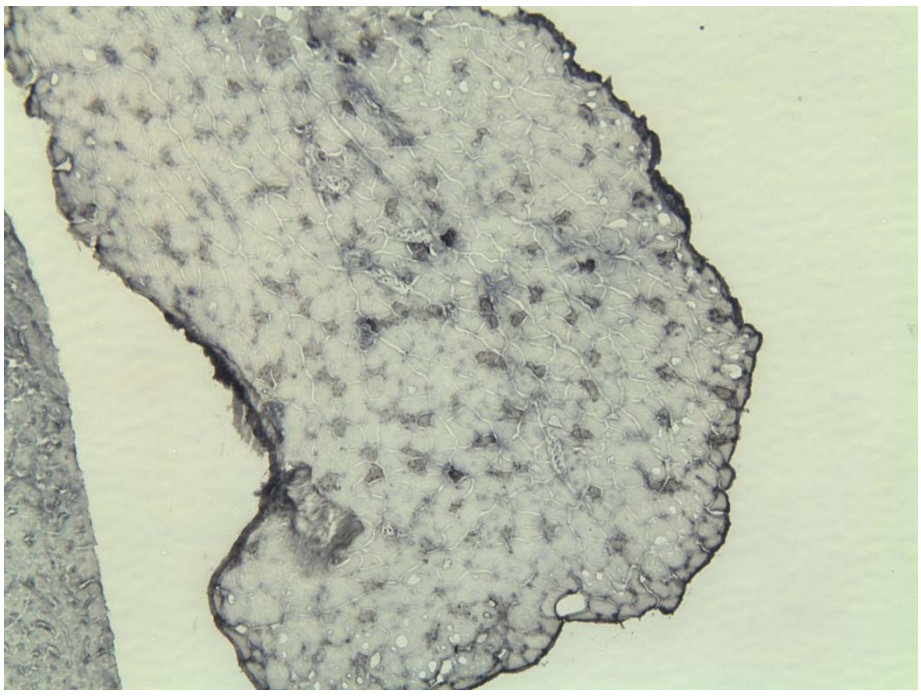

Figure 16. Slow Twitch (df5 L Sol, 10x)

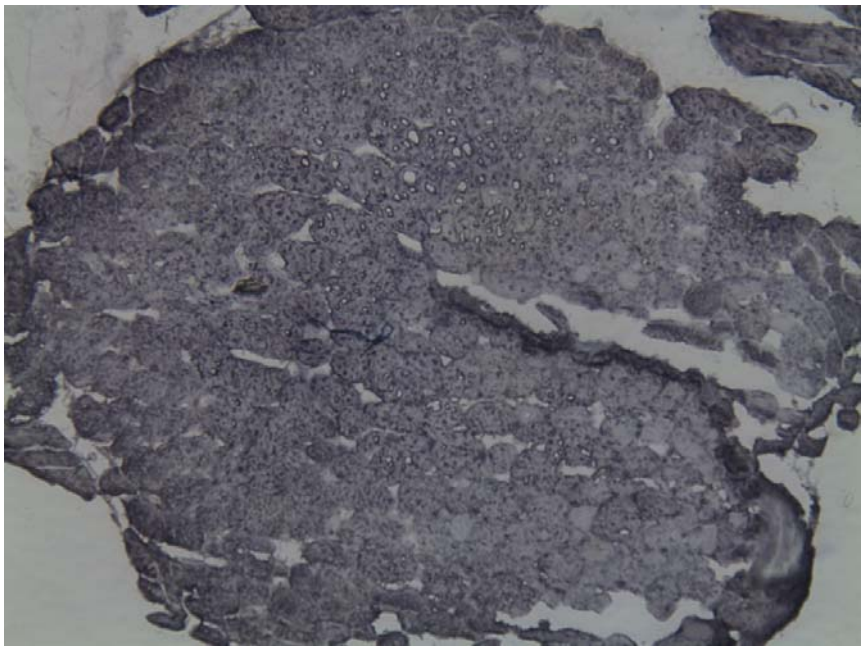

Figure 17. Fast Twitch (N3 R EDL, 10x)

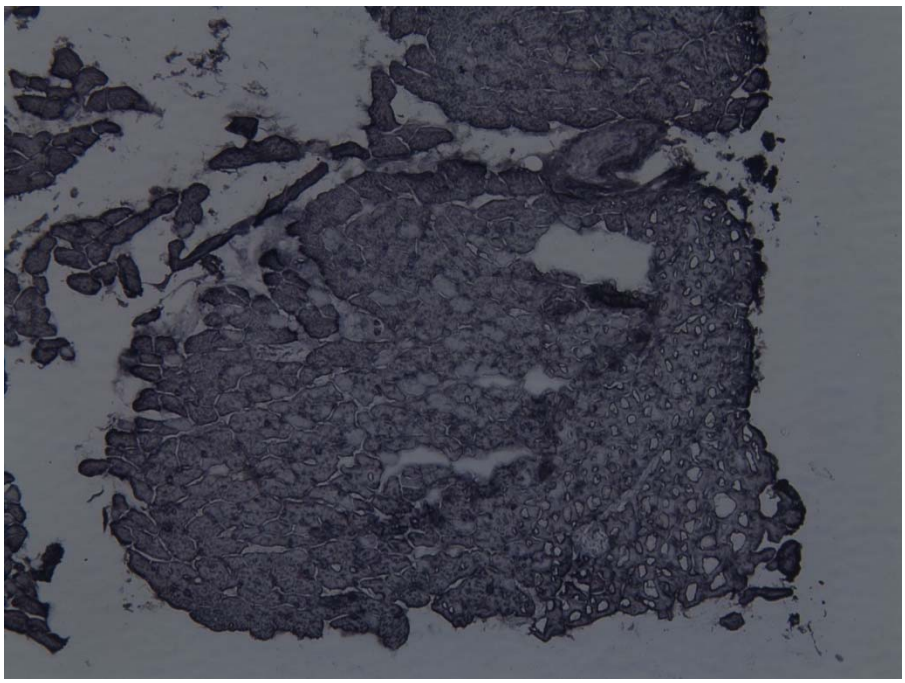

Figure 18. Fast Twitch (df5 R EDL, 10x)

CHAPTER IV

DISCUSSION

Utilizing research based on sarcopenia the researches expected the cellular diameter to decrease with the aged mice. The decrease would be greater with the normal mice compared to the dwarf mice due to the studied age resistance of the dwarf. Based on the structural sizes of the animals, the normal mouse was expected to have a larger cellular diameter when compared to the dwarf mouse. In addition, the EDL was expected to be a primary fast twitch muscle with the SOL being a primary slow twitch muscle. Based on the previous research of sarcopenia, researchers expected the fast twitch muscle fibers percentage to decrease with age in both mice.[10,22,23] A study analyzing the soleus skeletal muscle in rats found a 30% decrease in muscle cross-sectional area with age, after the rat was 36 months old.[24] Based on previous researching proving an increase in antioxidant defense, and extended life span of the dwarfs,[18,19,20] researchers expected to find a larger decrease in fast twitch muscle percentage compared to the Ames dwarf mice.

Based on the data collected during this study, researchers experienced a few unexpected significant findings following the completion of the cell circling data. A significant difference was found with the normal mice between 3 and 12 months, in which the 12 month normal mice had a larger cellular diameter, see

Figure 8 and Table 8. The sample size for the data is one mouse, with further research required to support this finding. This finding may be due to the issue that the 12 month mouse is not fully grown, researchers made the assumption that a 12 month mouse is an aged mouse, however, if the mouse was still growing this data would be expected. Further research is required in older mice (24 months) to see if there is a decrease in cellular diameter between the 3 month and 24 month as well as the 12 month and 24 month old mouse.

Throughout the study there were a few limitations that may have altered the results. Tissue weights and measurements were not obtained for all mice (Table 4) during the time of surgery due to altered protocol after surgeries were initiated. Staining supplies were found to be out of date; however, the tissue samples were removed from the freezer before this information was discovered, resulting in increased freeze-thaw times, maybe leading to tissue refraction and poor picture quality such as df4 and df5 in Table 9. Data collections during fast and slow twitch muscle fibers were obtained by non-blinded researchers; this counting was performed by both researchers which may have resulted in inconsistent counts because images were only counted by one researcher. The software utilized in cell circling had limitations because the program would automatically select a portion of the whole tissue image and would not allow alterations of the selected image, limiting the available cells to utilize during the analysis.

Further research is suggested to increase the sample size of the animals as well as the available age ranges, with a suggestion of utilizing mice age 24

months. Involving blinded researchers for the data collection of cell circling and fast and slow twitch counting is suggested to have unbiased data analyzed. In addition, future studies should analyze information from the other muscles collected in this study, tibialis anterior and gastrocnemius/plantaris.

REFERENCES

1. Abellan van Kan G. Epidemilogy and consequences of sarcopenia. *J Nutr Health Aging.* 2009;13:708-712.

2. Doherty TJ. Invited review: aging and sarcopenia. *J Appl Physiol.* 2003; 95:1717-1727.

3. Rosenberg I. Summary comments: epidemiological and methodological problems in determining nutritional status of older persons. *Am J Clin Nutr.* 1989;50:1231-1233.

4. Rosenberg IH. Sarcopenia: origins and clinical relevance. *J Nutr* 1997. 127:990S-991S.

5. Morely JE, Baumgartner RN, Roubenoff R et al. Sarcopenia. *J Lab Clin Med* 2001;137:231-243.

6. Cruz-Jentoft AJ, Baeyens JP, Bauer JM, Boirie Y, Cederholm T, Landi F, *et al.* European Working Group on Sarcopenia in Older People. Sarcopenia: European consensus on definition and diagnosis: report of the European Working Group on Sarcopenia in Older People. *Age Aging*. 2010;39:412-423.

7. Neumann DA. *Kinesiology of the Musculoskeletal System: Foundations for Rehabilation.* 2nd ed. St. Louis, Misso: Mosby Elsevier; 2010: 47-73.

8. Parts of a muscle. Skeletal Muscle. http://www.shoppingtrolley.net/skeletal%20muscle.shtml. Accessed April 11, 2011.

9. Sweeney LJ, Brodfuehrer PD, Raughley BL. An introductory biology lab that uses enzyme histochemistry to teach students about skeletal muscle fiber types. *Adv Physiol Educ* 2004; 28:23-28.

10. Lang T, Streeper T, Cawthon P, Baldwin K, Taaffe DR, Harris TB. Sarcopenia: etiology, clinical consequences, intervention and assessment. *Osteoporosis Int.* 2010; 21:543-559.

11. Roubenoff R, Hughes VA. Sarcopenia: Current Concepts. *J Gerontol.* 2000; 55:M716-26. Available from PubMed. Accessed April 20, 2011

12. Baumgartner RN, Koehler KM, Gallagher D, *et al.* Epidemiology of sarcopenia among the elderly in New Mexico. *Am J Epidemiol.* 1998;147: 755-763.

13. Venes D, *Taber's Cyclopedic Medical Dictionary.* 21st ed. Philadelphia, PA: FA Davis Co; 2005:1963.

14. Haran D. Aging: A theory based on free radical and radiation chemistry. *J Gerontology* 1956 11;298-300.

15. Finkel T. Signal transduction by reactive oxygen species. *J Cell Biol.* 2011 Jul 11;194(1):7-15.

16. Thompson LV. Age-related muscle dysfunction. *Exp Gerontol*. 2009; 44:106-111.

17. Sigak RS, Weindruch R. Oxidative stress, caloric restriction and aging. *Sci* 1996;273:59-63.

18. Brown-Borg HM, Rakoczy SG. Growth hormone administration to long-living dwarf mice alters multiple compnents of the antioxidative defense system. *Mech Age Dev*. 2003;124:1013-1024.

19. Romanick MA, Rakoczy SG, Brown-Borg HM. Long-lived Ames dwarf mouse exhibits increased antioxidant defense in skeletal muscle. *Mech Age Dev*. 2004;125:269-281.

20. Sharma S, Rakoczy S, Dahlheimer K, *et al.* The hippocampus of Ames dwarf mice exhibits enhanced antioxidant defenses following kainic acid-induced oxidative stress. *Exp Gerontol.* 2010;45:936-949.

21. Brown-Borg HM, Borg KE, Meliska CJ, *et al.* Dwarf mice and the ageing process. *Nature*. 1996;384:33.

22. Thompson LV. Effects of age, and training on skeletal muscle physiology and performance. *Phys Ther.* 74:71–81.

23. Von Haehling S, Morley JE, Anker SD. An overview of sarcopenia: facts and numbers on prevalence and clinical impact. *J Cachexia Sarcopenia Muscle.* 2010:1:129-133.

24. Thompson LV, Brown M. Age-related changes in contractile properties of single skeletal fibers from the soleus muscle. *J Appl Physiol.* 1999;86(3): 881-886.